

Approximating chiral $SU(3)$ amplitudes

G. Ecker¹, P. Masjuan² and H. Neufeld¹

¹) University of Vienna, Faculty of Physics, Boltzmanngasse 5, A-1090 Wien, Austria

²) Institut für Kernphysik, Johannes Gutenberg-Universität, D-55099 Mainz, Germany

Abstract

We construct large- N_c motivated approximate chiral $SU(3)$ amplitudes of next-to-next-to-leading order. The amplitudes are independent of the renormalization scale. Fitting lattice data with those amplitudes allows for the extraction of chiral coupling constants with the correct scale dependence. The differences between approximate and full amplitudes are required to be at most of the order of $N^3\text{LO}$ contributions numerically. Applying the approximate expressions to recent lattice data for meson decay constants, we determine several chiral couplings with good precision. In particular, we obtain a value for F_0 , the meson decay constant in the chiral $SU(3)$ limit, that is more precise than all presently available determinations.

1 Introduction

Hadronic processes at low energies cannot be treated with perturbative QCD. The main protagonists in this field, lattice QCD and chiral perturbation theory (CHPT), have mutually benefited from a cooperation started several years ago. The emphasis of this cooperation has shifted in recent years. Although extrapolation to the physical quark (and hadron) masses and finite-volume corrections, both accessible in CHPT, are still useful for lattice simulations, improved computing facilities and lattice algorithms allow for simulations with ever smaller quark masses and larger volumes. On the other hand, the input of lattice QCD for CHPT has become more important over the years to determine the coupling constants of chiral Lagrangians, the so-called low-energy constants (LECs). This input is especially welcome for LECs modulating quark mass terms: unlike in phenomenological analyses, quark (and hadron) masses can be tuned on the lattice.

While this program has been very successful for chiral $SU(2)$, the situation is less satisfactory for $SU(3)$ [1]. In the latter case, the natural expansion parameter (in the meson sector) is $M_K^2/16\pi^2 F_\pi^2 \simeq 0.2$. To match the precision that lattice studies can attain nowadays, it is therefore mandatory to include NNLO contributions in CHPT. Although NNLO amplitudes are available for most quantities of interest for lattice simulations [2], there has been a certain reluctance in the lattice community to make full use of those amplitudes for two reasons mainly: for chiral $SU(3)$, NNLO amplitudes are usually quite involved and they are mostly available in numerical form only.

In this paper, we resume our proposal [3] for large- N_c motivated approximations of NNLO amplitudes that contain one-loop functions only. Besides recapitulating the main features of those analytic approximations, the following issues will be discussed.

- We set up numerical criteria for the amplitudes to qualify as acceptable approximations. Those criteria can be checked by comparing with available numerical results making use of the full NNLO amplitudes for some given sets of meson masses.
- The proposed approximation includes all terms leading and next-to-leading order in large N_c . In addition, it contains all chiral logs, independently of the large- N_c counting. In order to meet the numerical criteria just mentioned, it may sometimes be useful to go beyond the strict large- N_c counting by including also products of one-loop functions occurring in two-loop diagrams.
- In addition to the ratio F_K/F_π of meson decay constants investigated in Ref. [3], here we also study the pion decay constant F_π itself. By confronting our approximation with lattice data, we demonstrate the possibilities to extract information on both NLO and NNLO LECs. While the NNLO LECs have the expected large uncertainties, the NLO LECs can be determined quite well. Our numerical fits of lattice data are not intended to compete with actual lattice results for obvious reasons. Instead, we hope to encourage lattice groups to use NNLO amplitudes that are much simpler than the full amplitudes and yet offer considerably more insight than, e.g., polynomial fits. These amplitudes can also be considered as relatively simple tools to study convergence issues of chiral $SU(3)$ with lattice data.

In Sec. 2 we review the structure and the salient features of the approximate form of NNLO amplitudes for chiral $SU(3)$ proposed in Ref. [3]. In addition to setting up a criterion

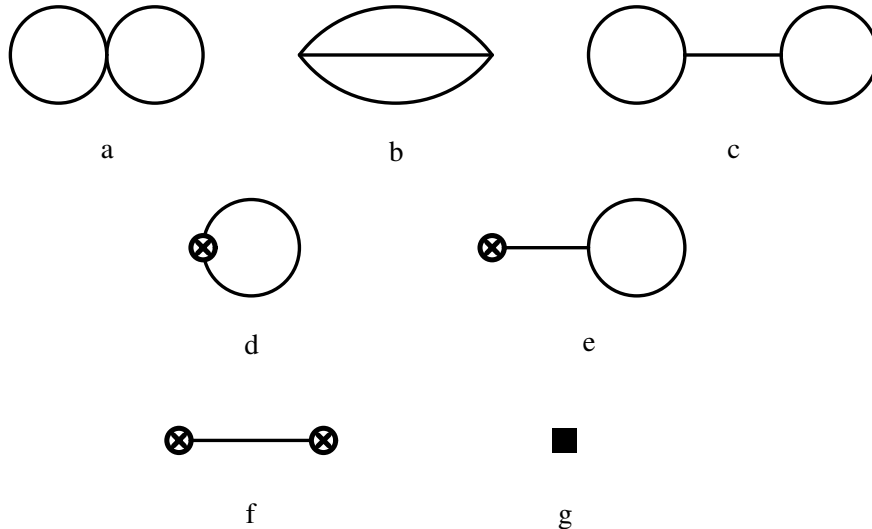


Figure 1: Skeleton diagrams for the generating functional Z_6 of $O(p^6)$. Simple dots, crossed circles, black box denote vertices from LO, NLO, NNLO Lagrangians, respectively. Propagators and vertices carry the full tree structure associated with the lowest-order Lagrangian.

for deciding whether the approximation is acceptable for a given observable, we also suggest a possible modification of the original version. Both approximations are applied to an analysis of lattice data for the ratio F_K/F_π to extract NLO and NNLO LECs. We study in detail the dependence of the approximations on a scale parameter M that mimics the neglected two-loop contributions. The extracted LECs are then used in Sec. 4 to analyse F_π in chiral $SU(3)$. It turns out that F_π is well suited for determining the leading-order LEC F_0 , the meson decay constant in the chiral $SU(3)$ limit. We demonstrate why the NLO LEC L_4 is usually strongly anti-correlated with F_0 in phenomenological analyses. We also discuss the constraints on F_0 coming from a comparison with chiral $SU(2)$. Sec. 5 contains a few remarks on the kaon semileptonic vector form factor at $t = 0$. In App. A we rederive the generating functional of Green functions at NNLO [4] in a form suitable for our analytic approximations. Explicit approximate expressions for F_K/F_π and F_π , which are the basis for the analysis in previous sections, are presented in Apps. B and C, respectively.

2 Analytic approximations of NNLO amplitudes

CHPT can be formulated in terms of the generating functional of Green functions $Z[j]$ [5, 6]. The NNLO functional Z_6 of $O(p^6)$ is a sum of various contributions shown in Fig. 1. In App. A, we derive an explicit representation of Z_6 based on the work of Ref. [4]. In Ref. [3],

we proposed an analytic approximation for Z_6 of the following form:

$$\begin{aligned}
Z_6^I &= \int d^4x \left\{ \left[C_a^r(\mu) + \frac{1}{4F_0^2} \left(4\Gamma_a^{(1)} L(\mu) - \Gamma_a^{(2)} L(\mu)^2 + 2\Gamma_a^{(L)}(\mu)L(\mu) \right) \right] O_a(x) \right. \\
&\quad \left. + \frac{1}{(4\pi)^2} \left[L_i^r(\mu) - \frac{\Gamma_i}{2} L(\mu) \right] H_i(x; M) \right\} \\
&\quad + \int d^4x d^4y \left\{ \left(L_i^r(\mu) - \frac{\Gamma_i}{2} L(\mu) \right) P_{i,\alpha}(x) G_{\alpha,\beta}(x, y) \left(L_j^r(\mu) - \frac{\Gamma_j}{2} L(\mu) \right) P_{j,\beta}(y) \right. \\
&\quad \left. + 2 \left(L_i^r(\mu) - \frac{\Gamma_i}{2} L(\mu) \right) P_{i,\alpha}(x) G_{\alpha,\beta}(x, y) F_\beta(y; M) \right\} . \tag{2.1}
\end{aligned}$$

The monomials $O_a(x)$ ($a = 1, \dots, 94$) define the chiral Lagrangian of $O(p^6)$ [7] with associated renormalized LECs $C_a^r(\mu)$ and the $L_i^r(\mu)$ ($i = 1, \dots, 10$) are renormalized LECs of $O(p^4)$ with associated beta functions Γ_i [6]. The coefficients $\Gamma_a^{(1)}$, $\Gamma_a^{(2)}$ and $\Gamma_a^{(L)}$ are listed in Ref. [4]. Repeated indices are to be summed over. F_0 is the meson decay constant in the chiral $SU(3)$ limit. The chiral log

$$L(\mu) = \frac{1}{(4\pi)^2} \ln M^2/\mu^2 \tag{2.2}$$

involves an arbitrary scale M . This scale is introduced in the complete functional Z_6 in Eq. (A.21) to make the scale dependence explicit: only $C_a^r(\mu)$, $L_i^r(\mu)$ and $L(\mu)$ in (2.1) depend on the renormalization scale μ . The various functionals in Eq. (2.1) are defined in App. A. The approximation consists in dropping in Z_6 the irreducible two-loop contributions represented by the functional $K(x; M)$ (diagrams a,b in Fig. 1) and the terms bilinear in $F_\alpha(x; M)$ (diagram c in Fig. 1), except for single and double logs.

The procedure how to actually calculate an amplitude corresponding to Eq. (2.1) was described in Ref. [3]. In many cases, the relevant amplitudes can be extracted from available calculations of $O(p^6)$ [2].

Approximation I defined by Eq. (2.1) has the following properties [3]:

- All chiral logs are included.
- The functional Z_6^I is independent of the renormalization scale μ . Unlike the double-log approximation [8], it therefore allows for the extraction of LECs with the correct scale dependence.
- In addition to single and double logs, the residual dependence on the scale M is the only other vestige of the two-loop part.
- In dropping the genuine two-loop contributions, Approximation I respects the large- N_c hierarchy of $O(p^6)$ contributions:

$$C_a, L_i L_j \quad \longrightarrow \quad L_i \times \text{loop} \quad \longrightarrow \quad \text{two-loop contributions}$$

- Only tree and one-loop amplitudes need to be calculated.

The question still remains to be answered how reliable this approximation is. We shall adopt the following criterion. For an $SU(3)$ quantity normalized to one at lowest order, successive terms in the chiral expansion usually show the following generic behaviour:

$$\begin{array}{ccc}
O(p^4) & O(p^6) & O(p^8) \\
\lesssim 0.3 & \lesssim 0.3^2 = 0.09 & \lesssim 0.3^3 = 0.027
\end{array}$$

This suggests as a criterion for an acceptable NNLO approximation that the accuracy should not be worse than 3 %, the typical size of contributions of $O(p^8)$. As the following examples will show, the quality of the approximation depends on the scale M , which parametrizes the two-loop contributions not contained in (2.1). Although the acceptable range will depend on the quantity under consideration, experience with the double-log approximation [8] in chiral $SU(3)$ suggests that M is of the order of M_K .

Approximation I is motivated by large N_c , but in some cases the accuracy may be improved by including in the approximate functional (2.1) also products of one-loop amplitudes (diagrams a,c in Fig. 1, subleading in $1/N_c$), which also have a simple analytic form. We call this extension Approximation II. In contrast to Approximation I, this extension is not uniquely defined¹ because it depends on the representation of the matrix field U . In the standard representation used, e.g., also in Refs. [4, 9], it amounts to omitting (except for chiral logs) the sunset diagram b from the full functional Z_6 in Eq. (A.21).

3 F_K/F_π and the low-energy constant L_5

The ratio of pseudoscalar decay constants F_K/F_π appears well suited for our analytic approximations. The chiral expansion of $F_K/F_\pi - 1$ is shown for physical meson masses in Table 1. The separately scale-dependent contributions of $O(p^6)$ are given for the usual renormalization scale $\mu = 770$ MeV. The entries for “numerical results” were provided by Bernard and Passemar [10].

	$O(p^4)$	$O(p^6)$		
		2-loop	$L_i \times \text{loop}$	tree
numerical results [9, 10]	0.14	0.002	0.051	0.008
Approximation I ($M = M_K$)		- 0.030		
Approximation II ($M = M_K$)		- 0.011		

Table 1: Chiral expansion of $F_K/F_\pi - 1$. The separate contributions of $O(p^6)$ are listed for $\mu = 770$ MeV.

As shown in Table 1, Approximation I barely meets our criterion of acceptability put forward at the end of the last section, while Approximation II does much better. To investigate also the dependence on the scale M , we display in Fig. 2 the variation with M for both versions I and II and for two sets of meson masses. As demonstrated in Fig. 2, there is little dependence

¹Hans Bijmans, private communication

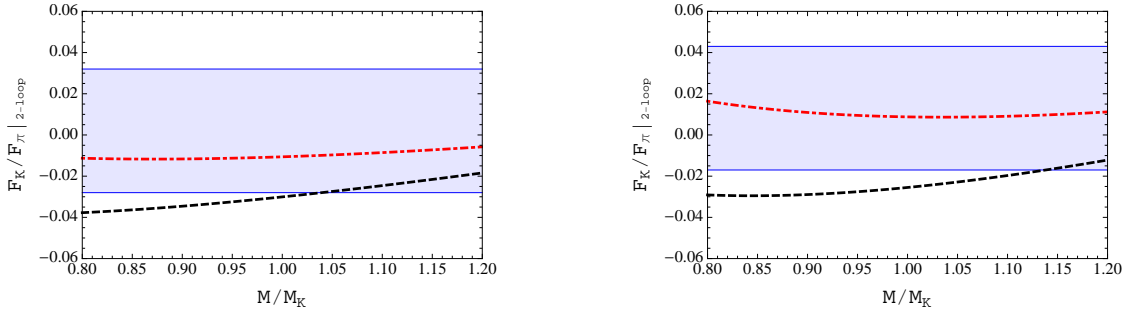


Figure 2: M -dependence of Approximations I, II for the two-loop contributions to F_K/F_π at $\mu = 770$ MeV. The blue bands denote the $\pm 3\%$ regions around the actual values provided by Bernard and Passemar [10]. The dashed black curves correspond to Approximation I, the dash-dotted red curves to Approximation II. The left panel describes the situation for physical meson masses, the right panel for masses $M_\pi = 416$ MeV, $M_K = 604$ MeV.

on M in the vicinity of $M = M_K$. Nevertheless, we will account for this variation in the final errors for the preferred Approximation II.

The explicit expression for Approximation II of F_K/F_π is given in App. B where all masses are lowest-order masses of $O(p^2)$. Since we work to $O(p^6)$ the masses in R_4 must be expressed in terms of the lattice masses to $O(p^4)$ [6]. The chiral limit value F_0 is expressed in terms of the experimental value $F_\pi = 92.2$ MeV and physical meson masses, using again the $O(p^4)$ relation. In R_6 and R_6^{ext} , F_0 and the meson masses can be replaced by F_π and lattice masses, respectively.

We now repeat the analysis of F_K/F_π performed in Ref. [3] with Approximation II. We recall that at $O(p^4)$ only the LEC L_5 enters. At $O(p^6)$, two combinations of NNLO LECs appear: $C_{14} + C_{15}$ and $C_{15} + 2C_{17}$. At this order, also some of the L_i enter, but only the term with L_5^2 is leading in $1/N_c$. In the spirit of large N_c , we therefore extract as in Ref. [3] L_5 , $C_{14} + C_{15}$ and $C_{15} + 2C_{17}$ from a fit of the lattice data of the BMW Collaboration [11], using for the remaining L_i (appearing only at $O(p^6)$, subleading in $1/N_c$) the values of fit 10 of Ref. [12]. The results are displayed in Table 2.

	F_K/F_π	$10^3 L_5^r$	$10^3(C_{14}^r + C_{15}^r)$	$10^3(C_{15}^r + 2C_{17}^r)$
App. I ($M = M_K$)	1.198(5)	0.76(8)	0.37(7)	1.29(14)
App. II	1.200(5)	0.75(8)	0.20(8)	0.71(22)
BMW [11]	1.192(7) _{stat} (6) _{syst}			

Table 2: Fit results for F_K/F_π and LECs for Approximations I (statistical errors only) and II. The renormalization scale is $\mu = 770$ MeV for all LECs. The LECs C_a^r have dimension GeV^{-2} .

The fitted values of F_K/F_π agree with the detailed analysis of Ref. [11]. For both F_K/F_π and L_5 , there is practically no difference between the two approximations but the LECs of $O(p^6)$ show a bigger spread. For Approximation II, we have added the uncertainty due to varying

M in the range $0.9 \leq M/M_K \leq 1.1$ in quadrature to the statistical lattice errors. The effect of this variation is small, for F_K/F_π and L_5 in fact negligible. Since C_{15} is subleading in $1/N_c$ the fit determines essentially C_{14} and C_{17} [10]. Although the values depend of course on the input for the L_i , the results in Table 2 suggest that both C_{14}^r and C_{17}^r are positive and smaller than 10^{-3} GeV^{-2} , always taken at $\mu = 0.77 \text{ GeV}$. We will use these fit results with Approximation II for L_5^r , C_{14}^r and C_{17}^r in the analysis of F_π/F_0 in the following section.

The fit also demonstrates very clearly that NNLO terms are essential. While the NNLO fit (Approximation II) is well behaved ($\chi^2/\text{dof} = 1.2$, statistical errors only), the NLO fit with the single parameter L_5 is unacceptable ($\chi^2/\text{dof} = 4$). Analysing present-day lattice data with NLO chiral $SU(3)$ expressions does not make sense.

4 F_π and the low-energy constants F_0, L_4

The meson decay constant in the chiral limit is a LEC of the lowest-order chiral Lagrangian. In the case of chiral $SU(2)$, $F = \lim_{m_u, m_d \rightarrow 0} F_\pi$ is well known, mainly from a combined analysis of lattice data with $N_f = 2$ active flavours by the FLAG Collaboration [1]:

$$F = (85.9 \pm 0.6) \text{ MeV} . \quad (4.1)$$

The situation is quite different in the $SU(3)$ case. The lattice results for $F_0 = \lim_{m_u, m_d, m_s \rightarrow 0} F_\pi$ cover a much wider range, from about 66 MeV to 84 MeV [1]. A similar range is covered in the phenomenological fits of Bijmans and Jemos [13].

The low-energy expansion in chiral $SU(3)$ is characterized by the ratio $p^2/(4\pi F_0)^2$ where p stands for a generic meson momentum or mass. F_0 thus sets the scale for the chiral expansion. In practice, F_0 is usually traded for F_π at successive orders of the chiral expansion. Nevertheless, F_0 affects the ‘‘convergence’’ of the chiral expansion: a smaller F_0 tends to produce bigger fluctuations at higher orders.

Why has it been so difficult both for lattice and phenomenological studies to determine F_0 ? One clue is the apparent anti-correlation with the NLO LEC L_4 in the fits of Ref. [13]: the bigger F_0 , the smaller $L_4^r(M_\rho)$, and vice versa. The large- N_c suppression of L_4 is not manifest in the fits with small F_0 .

This anti-correlation can be understood to some extent from the structure of the chiral $SU(3)$ Lagrangian up to and including NLO:

$$\begin{aligned} \mathcal{L}_{p^2}(2) + \mathcal{L}_{p^4}(10) &= \frac{F_0^2}{4} \langle D_\mu U D^\mu U^\dagger + \chi U^\dagger + \chi^\dagger U \rangle + L_4 \langle D_\mu U D^\mu U^\dagger \rangle \langle \chi U^\dagger + \chi^\dagger U \rangle + \dots \\ &= \frac{1}{4} \langle D_\mu U D^\mu U^\dagger \rangle \left[F_0^2 + 8L_4 \left(2\overset{\circ}{M}_K^2 + \overset{\circ}{M}_\pi^2 \right) \right] + \dots \end{aligned} \quad (4.2)$$

The unitary matrix field U is parametrized by the meson fields, $\chi = 2B_0\mathcal{M}_q$ ($B_0 \sim$ quark condensate, \mathcal{M}_q is the quark mass matrix), $\langle \dots \rangle$ stands for the $SU(3)$ flavour trace and $\overset{\circ}{M}_P$ denotes the lowest-order meson masses. The dots refer to the remainder of the NLO Lagrangian in the first line and to terms of higher order in the meson fields in the second line. Therefore, a LO tree-level contribution is always accompanied by an L_4 contribution in the combination

$$F(\mu)^2 := F_0^2 + 8L_4^r(\mu) \left(2\overset{\circ}{M}_K^2 + \overset{\circ}{M}_\pi^2 \right) . \quad (4.3)$$

Of course, there will in general be additional contributions involving L_4 at NLO, especially in higher-point functions (e.g., in meson meson scattering). Nevertheless, the observed anti-correlation between F_0 and L_4 is clearly related to the structure of the chiral Lagrangian. Note that $F_\pi^2/16M_K^2 = 2 \times 10^{-3}$ is the typical size of a NLO LEC. Although of different chiral order, the two terms in $F(\mu)^2$ could a priori be of the same order of magnitude.

Independent information on F_0 comes from comparing the $SU(2)$ and $SU(3)$ expressions for F_π . To $O(p^4)$ in chiral $SU(2)$, F_π is given by [5]

$$F_\pi = F + F^{-1} [M_\pi^2 l_4^i(\mu) + \bar{A}(M_\pi, \mu)] \quad (4.4)$$

where l_4 is a NLO $SU(2)$ LEC and $\bar{A}(M_\pi, \mu)$ is a one-loop function defined in Eq. (B.5). Expressing $l_4^i(\mu)$ in terms of $L_4^r(\mu)$, $L_5^r(\mu)$ and a kaon loop contribution [6] and equating Eq. (4.4) with the $SU(3)$ result for F_π , one arrives at the following relation:

$$F_0 = F - F^{-1} \left\{ (2M_K^2 - M_\pi^2) \left(4L_4^r(\mu) + \frac{1}{64\pi^2} \ln \frac{\mu^2}{M_K^2} \right) + \frac{M_\pi^2}{64\pi^2} \right\} + O(p^6). \quad (4.5)$$

To $O(p^6)$, the relation between F_0 and F was derived by Gasser et al. [14]. It depends on LECs of both NLO and NNLO. In Fig. 4, both $O(p^4)$ and $O(p^6)$ relations will be displayed. Of course, in order to plot F_0 as a function of L_4 to $O(p^6)$, some assumptions about NLO and NNLO LECs are needed.

$SU(3)$ lattice data for F_π seem well suited for a determination of F_0 and L_4 although the emphasis in most lattice studies has been to determine F_π itself. As for F_K/F_π , the use of CHPT to NNLO, $O(p^6)$ [9], is essential for a quantitative analysis.

In the following, we are going to apply Approximation I for the analysis of F_π . It turns out that, unlike for F_K/F_π , Approximation I agrees better with the numerical results of Ref. [10] than Approximation II. The explicit representation for F_π is given in App. C. The lowest-order masses appearing in the terms of $O(p^4)$ must again be expressed in terms of lattice masses. Unlike in the previous section, we leave F_0 in Eq. (C.1) untouched.

Again in contrast to the ratio F_K/F_π , the dependence on the mass parameter M is more pronounced in this case, especially for larger meson masses (see Fig. 3). To satisfy the requirement that our approximation should stay within $\pm 3\%$ of the exact numerical results [10], we are going to vary M in the range $0.97 \leq M/M_K \leq 1.09$.

In addition to F_0 and L_4 , the only other LEC appearing to $O(p^4)$ in Eq. (C.1) is L_5 . On the basis of the analysis of F_K/F_π in Sec. 3, we will use $L_5^r = (0.75 \pm 0.10) \cdot 10^{-3}$. At $O(p^6)$, the following NNLO LECs enter: C_{14} , C_{15} , C_{16} and C_{17} , but only C_{14} and C_{17} are leading in $1/N_c$. In the spirit of large N_c , we therefore use the values for C_{14} and C_{17} obtained in the previous section, neglecting at the same time C_{15} and C_{16} . However, we assign a 100 % uncertainty to both C_{14} and C_{17} . Anticipating the dependence of the relation between F_0 and F at $O(p^6)$ on C_{16} [14] in Fig. 4, we include for consistency the uncertainty due to varying $C_{16}^r(M_\rho)$ between $\pm C_{14}^r(M_\rho)$. At $O(p^6)$, some more of the NLO LECs L_i enter. For definiteness, we use again fit 10 of Ref. [12] for those LECs. However, any other set of values for the L_i from Refs. [12, 13] consistent with large N_c , in particular with a small $L_4^r(M_\rho)$, leads to very similar results.

We confront the expression (C.1) for F_π with lattice data from the RBC/UKQCD Collaboration [15, 16]. In our main fit we only consider (five) unitary lattice points with $M_\pi < 350$

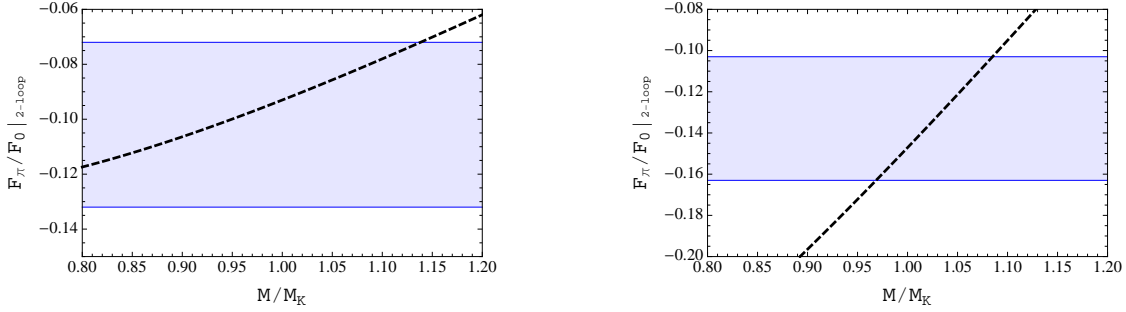


Figure 3: M -dependence of Approximation I for the two-loop contributions to F_π at $\mu = 770$ MeV (dashed black curves). The blue bands denote the $\pm 3\%$ regions around the actual values provided by Bernard and Passemar [10]. The left panel describes the situation for physical meson masses, the right panel for masses $M_\pi = 416$ MeV, $M_K = 604$ MeV.

MeV. In this case, F_π for physical meson masses emerges as a fit result but the fitted value is lower than the experimental value. Another alternative is therefore to use in addition to the lattice points also the experimental value $F_\pi = (92.2 \pm 0.3)$ MeV as input where we have doubled the error assigned by the Particle Data Group [17].

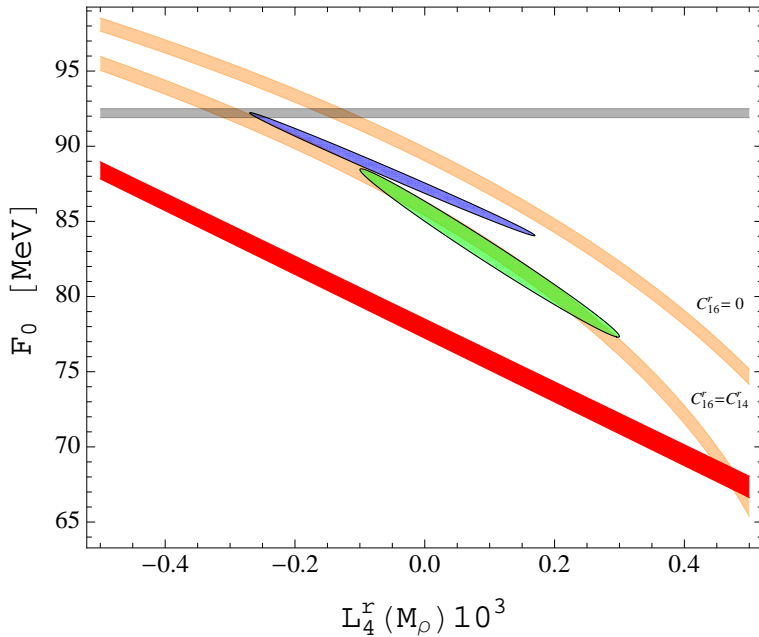


Figure 4: Fitted values of F_0 , L_4 using RBC/UKQCD data [15, 16] with $M_\pi < 350$ MeV, with (blue ellipse) and without (green ellipse) including F_π^{phys} . The red band results from the comparison of F_π between $SU(2)$ and $SU(3)$ as expressed by Eq. (4.5), taking $F = (85.9 \pm 0.6)$ MeV [1]. The relation between F_0 and F to $O(p^6)$ [14] leads to the orange bands for two values of $C_{16}^r(M_\rho)$. The horizontal grey band denotes $F_\pi = (92.2 \pm 0.3)$ MeV.

The extracted values of F_0 and $L_4^r(M_\rho)$ are shown in Fig. 4. For the case where F_π^{phys} is

included (blue ellipse), the explicit fit results are:

$$\begin{aligned}
F_0 &= (88.1 \pm 4.1) \text{ MeV} \\
10^3 L_4^r(M_\rho) &= -0.05 \pm 0.22 \\
\text{corr}(F_0, L_4^r) &= -0.996 .
\end{aligned}
\tag{4.6}$$

The errors of F_0 , L_4 are due to both lattice and theoretical uncertainties. First, there are statistical errors of the lattice values for F_π and the meson masses and, in addition, the uncertainties of the inverse lattice spacings. The dominant errors are those of the lattice spacings and of F_π , whereas the errors of the lattice masses are practically negligible. We have neglected unknown correlations among the lattice data, thereby probably overestimating the combined errors.

In addition, we added the theoretical uncertainties related to M , L_5 and the C_a in quadrature. Lattice and theoretical errors are of similar size. For instance, keeping only the lattice errors, the error of F_0 moves from 4.1 down to 2.8 MeV. The χ^2/dof is 0.5 (statistical errors only), suggesting once more that we have at least not underestimated the errors.

The two ellipses are roughly compatible with each other. The green ellipse is lower because from the RBC/UKQCD data alone the fitted value of F_π is smaller than the experimental value. The value for L_4 is consistent with large N_c and with available lattice results [1]. The result for F_0 is more precise than existing phenomenological and lattice determinations. It is somewhat bigger than expected [18], roughly of the same size as the $SU(2)$ LEC F in Eq. (4.1).

F_0 and L_4 in Eq. (4.6) are compatible with the comparison between $SU(2)$ and $SU(3)$ to $O(p^6)$ [14], as indicated by the orange bands in Fig. 4. C_{16} is the only NNLO LEC appearing in the relation between F_0 and F . As always in this paper, we have used fit 10 [12] for the NLO LECs. However, unlike for our fit results (4.6), the orange bands in Fig. 4 are rather sensitive to the precise values of the L_i^r . Therefore, although the consistency between the ellipses and the lower orange band is manifest, it can hardly be used as a determination of C_{16} .

Raising the range in pion masses to $M_\pi < 425$ MeV, two more lattice points [15] can be added. Repeating the fit with the bigger sample moves the ellipses down, because with the original data set of RBC/UKQCD the fitted value of F_π comes out too low [15].

The strong anti-correlation between F_0 and L_4 persists because the kaon masses in the RBC/UKQCD data are all close to the physical kaon mass. Simulations with smaller kaon masses would not only be welcome from the point of view of convergence of the chiral series [19], but they could also provide a better lever arm for reducing the anti-correlation and the fit errors of F_0 and L_4 . This expectation is supported by the fact that the quantity $F(M_\rho)$ defined in Eq. (4.3) can be determined much better than F_0 .

5 Remarks on $\mathbf{f}_+^{\text{K}\pi}(0)$

The kaon semileptonic vector form factor at $t = 0$ is a crucial quantity for a precision determination of the CKM matrix element V_{us} . Both approximations discussed here do not appear very promising in this case.

First of all, unlike for F_π and F_K/F_π , the chiral expansion of $f_+^{K\pi}(0)$ shows a rather atypical behaviour. Due to the Ademollo-Gatto theorem [20], the $O(p^4)$ contribution of -0.0227 [21] is very small. On the basis of recent lattice studies, which find $f_+^{K\pi}(0) = 0.967$ with errors of less than 1% [22, 23], all higher-order contributions in CHPT would have to sum up to about -1% . On the other hand, the genuine two-loop contributions at the usual scale $\mu = 770$ MeV are positive and slightly bigger than 1% [10, 24, 25], suggesting that the remainder is about -2% to match the lattice value. In other words, the remainder would have to be as big as the NLO contribution, certainly not the typical behaviour for a chiral expansion.

In principle, Approximation I fulfills our criterion of Sec. 2 in differing from the full two-loop result [10, 24, 25] by less than 2%. However, especially in view of the accuracy of recent lattice studies claiming a precision of better than 1% for $f_+^{K\pi}(0)$, the accuracy of Approximation I is simply not sufficient in this case. Approximation II does not improve the situation.

To sum up, lattice determinations of $f_+^{K\pi}(0)$ seem to be able to do without CHPT. Moreover, only the full NNLO expression may allow for a meaningful extraction of LECs if at all [10].

6 Conclusions

We summarize the main results of our work.

1. Lattice QCD has become a major source of information for the low-energy constants of CHPT. We have argued that the meson decay constants F_π , F_K are especially suited for extracting chiral $SU(3)$ LECs of different chiral orders. The ratio F_K/F_π allows for a precise and stable determination of the NLO LEC L_5 . In addition, it gives access to some NNLO LECs although the accuracy is of course more limited in that case. Phenomenological analyses have had difficulties in determining the LEC F_0 , the meson decay constant in the chiral $SU(3)$ limit. We have shown that lattice data for F_π allow for the extraction of F_0 together with the NLO LEC L_4 . The strong anti-correlation between F_0 and L_4 observed in phenomenological analyses can in principle be lifted by varying the lattice masses. From a fit to the RBC/UKQCD data for F_π , we have obtained a value for F_0 that is more precise than other presently available determinations.
2. Confronting present-day lattice data with chiral $SU(3)$ requires chiral amplitudes to NNLO in most cases. Chiral $SU(3)$ amplitudes are often rather unwieldy and mostly available in numerical form only. We have therefore proposed large- N_c motivated approximate NNLO amplitudes that contain only one-loop functions. Unlike simpler approximations as the double-log approximation, our amplitudes are independent of the renormalization scale and can therefore be used to extract LECs with the correct scale dependence. However, approximations of NNLO amplitudes can only be successful if the differences to the full amplitudes are at most of the order of N³LO contributions. We have checked that this criterion can be fulfilled with our approximate amplitudes both for F_π and F_K/F_π . Therefore, we expect our results for the different LECs to be as reliable as CHPT to NNLO, $O(p^6)$, permits. Although our general criterion is also

satisfied for the kaon semileptonic form factor at $t = 0$, the approximate expression for $f_+^{K\pi}(0)$ is not precise enough compared to recent lattice data.

The main purpose of this work has been to encourage lattice groups to use NNLO amplitudes in chiral $SU(3)$ that are more user friendly than the full expressions and yet are reliable enough to provide more insight than NLO amplitudes with polynomial corrections.

Acknowledgements We are grateful to Véronique Bernard, Claude Bernard, Gilberto Colangelo, Laurent Lellouch, Heiri Leutwyler, Emilie Passemar and Lothar Tiator for helpful comments and suggestions. We are indebted to Elvira Gámiz for helping us to understand lattice data. Special thanks are due to Hans Bijmans for suggesting several substantial improvements of the original manuscript and for making the full results of Ref. [9] accessible to us. P.M. acknowledges support from the Deutsche Forschungsgemeinschaft DFG through the Collaborative Research Center “The Low-Energy Frontier of the Standard Model” (SFB 1044).

A Generating functional of $O(p^6)$

In this appendix we rederive the generating functional of $O(p^6)$ in the form used in Ref. [3]. It is a more explicit version of the derivation in Ref. [4].

The generating functional Z_6 is shown pictorially in Fig. 1. The various contributions to Z_6 are always understood as functionals of the classical field, the solution of the lowest-order field equations.

As discussed in Ref. [4], the sum of the reducible diagrams c, e, f leads to a finite and scale independent functional with the conventional choice of chiral Lagrangians. The contributions from diagrams a, b and d are divergent. The sum Z_6^{a+b+d} is still divergent, but the divergence takes the form of a local functional that is canceled by the divergent part of the tree-level functional Z_6^g in terms of the LECs C_a of $O(p^6)$.

We first consider the irreducible two-loop diagrams a, b. In d dimensions, the corresponding functional has the form

$$Z_6^{a+b} = \int d^d x (c\mu)^{2(d-4)} \left\{ \Lambda^2 \sum_a \alpha_a O_a(x) + \frac{\Lambda}{(4\pi)^2} \left[\sum_a (\beta_a + \alpha_a \ln M^2/\mu^2) O_a(x) + D(x; M) \right] + \frac{1}{(4\pi)^4} \left[E(x; M) + \ln^2 M^2/\mu^2 \sum_a \frac{\alpha_a}{2} O_a(x) + \ln M^2/\mu^2 \left(\sum_a \beta_a O_a(x) + D(x; M) \right) \right] \right\} \quad (\text{A.1})$$

with the divergence factor

$$\Lambda = \frac{1}{(4\pi)^2(d-4)}. \quad (\text{A.2})$$

The monomials $O_a(x)$ ($a = 1, \dots, 94$) define the chiral $SU(3)$ Lagrangian of $O(p^6)$ [7]. $D(x; M)$ and $E(x; M)$ are nonlocal functionals. The mass M is introduced to make the

dependence on the renormalization scale μ explicit. At this stage, the functional Z_6^{a+b} is independent of M . The scheme dependent constant c is conventionally chosen as in Eq. (2.22) of Ref. [4]. Eq. (A.1) is equivalent to Eq. (2.39) in Ref. [4] but the renormalization group equations (2.40) [4] have already been taken into account. In other words, the scale independence of Z_6^{a+b} is made explicit implying

$$\begin{aligned} \mu \frac{\partial \alpha_a}{\partial \mu} &= 0, & \mu \frac{\partial \beta_a}{\partial \mu} &= 0 \\ \mu \frac{\partial D(x; M)}{\partial \mu} &= 0, & \mu \frac{\partial E(x; M)}{\partial \mu} &= 0. \end{aligned} \quad (\text{A.3})$$

The general structure of the irreducible one-loop functional d is

$$Z_6^d = \int d^d x (c\mu)^{(d-4)} \sum_{i=1}^{10} L_i(d) Y_i(x, d) \quad (\text{A.4})$$

where the LECs of $O(p^4)$ are decomposed as

$$L_i(d) = (c\mu)^{d-4} [\Gamma_i \Lambda + L_i^r(\mu, d)] . \quad (\text{A.5})$$

Adopting the renormalization conventions of Ref. [4], the LECs $L_i^r(\mu, d)$ are not expanded around $d = 4$. Scale independence of the $L_i(d)$ then implies

$$\mu \frac{\partial L_i^r(\mu, d)}{\partial \mu} = -\frac{\Gamma_i}{(4\pi)^2} - (d-4)L_i^r(\mu, d) . \quad (\text{A.6})$$

Because of the divergence in $L_i(d)$ one must keep track of terms of $O(d-4)$ in $Y_i(x, d)$. With hindsight, these functionals can be written as

$$\begin{aligned} Y_i(x, d) &= \left(\Lambda + \frac{1}{2(4\pi)^2} \ln M^2/\mu^2 \right) \sum_a \eta_a^i O_a(x) \\ &+ \frac{1}{(4\pi)^2} \left\{ H_i(x, d; M) + (d-4) \left[\frac{1}{8} \ln^2 M^2/\mu^2 \sum_a \eta_a^i O_a(x) + \frac{1}{2} \ln M^2/\mu^2 H_i(x, d; M) \right] \right\} . \end{aligned} \quad (\text{A.7})$$

The scale independence of $(c\mu)^{d-4} Y_i(x, d)$ implies that the coefficients η_a^i are scale independent and that the functionals $H_i(x, d; M)$ satisfy the renormalization group equations

$$\mu \frac{\partial H_i(x, d)}{\partial \mu} = O[(d-4)^2] . \quad (\text{A.8})$$

Putting everything together, we obtain (using for convenience from now on the summation convention for both indices a, i)

$$\begin{aligned} Z_6^d &= \int d^d x (c\mu)^{2(d-4)} \left\{ \Lambda^2 \Gamma_i \eta_a^i O_a(x) \right. \\ &+ \frac{\Lambda}{(4\pi)^2} \left[(4\pi)^2 L_i^r(\mu, d) \eta_a^i O_a(x) + \frac{1}{2} \ln M^2/\mu^2 \Gamma_i \eta_a^i O_a(x) + \Gamma_i H_i(x, d; M) \right] \\ &+ \frac{1}{(4\pi)^4} \left[\frac{1}{8} \ln^2 M^2/\mu^2 \Gamma_i \eta_a^i O_a(x) + \frac{1}{2} \ln M^2/\mu^2 \Gamma_i H_i(x, 4; M) \right. \\ &\left. \left. + \frac{1}{2} \ln M^2/\mu^2 (4\pi)^2 L_i^r(\mu, 4) \eta_a^i O_a(x) + (4\pi)^2 L_i^r(\mu, 4) H_i(x, 4; M) \right] + O(d-4) \right\} . \end{aligned} \quad (\text{A.9})$$

Altogether, the irreducible contributions sum up to the functional

$$\begin{aligned}
Z_6^{a+b+d} &= \int d^d x (c\mu)^{2(d-4)} \left\{ \Lambda^2 [\alpha_a + \Gamma_i \eta_a^i] O_a(x) \right. \\
&+ \frac{\Lambda}{(4\pi)^2} \left[\beta_a O_a(x) + \ln M^2/\mu^2 \left(\alpha_a + \frac{1}{2} \Gamma_i \eta_a^i \right) O_a(x) \right. \\
&+ D(x; M) + \Gamma_i H_i(x, d; M) + (4\pi)^2 L_i^r(\mu, d) \eta_a^i O_a(x) \left. \right] \\
&+ \frac{1}{(4\pi)^4} \left[E(x; M) + \ln^2 M^2/\mu^2 \frac{\alpha_a}{2} O_a(x) + \ln M^2/\mu^2 (\beta_a O_a(x) + D(x; M)) \right. \\
&+ \frac{1}{8} \ln^2 M^2/\mu^2 \Gamma_i \eta_a^i O_a(x) + \frac{1}{2} \ln M^2/\mu^2 \Gamma_i H_i(x, 4; M) \\
&\left. + \frac{1}{2} \ln M^2/\mu^2 (4\pi)^2 L_i^r(\mu, 4) \eta_a^i O_a(x) + (4\pi)^2 L_i^r(\mu, 4) H_i(x, 4; M) \right] + O(d-4) \left. \right\} .
\end{aligned} \tag{A.10}$$

The double-pole divergence functional is automatically local. In order to cancel the divergences with the local functional Z_6^g , also the single-pole divergences in (A.10) must be local. Absence of the logarithmic terms implies the 94 Weinberg conditions [26]

$$\alpha_a = -\frac{1}{2} \Gamma_i \eta_a^i . \tag{A.11}$$

Moreover, the non-local functional $D(x; M)$ must be canceled by $\Gamma_i H_i(x, 4; M)$. More precisely, renormalization theory requires that

$$D(x; M) + \Gamma_i H_i(x, 4; M) = \Delta\beta_a O_a(x) , \tag{A.12}$$

i.e., that the sum of the two terms is local. In Ref. [4] it was found that the cancellation is complete: $\Delta\beta_a = 0$.

Using Eqs. (A.11) and (A.12) (with $\Delta\beta_a = 0$), the irreducible functional is given by

$$\begin{aligned}
Z_6^{a+b+d} &= \int d^d x (c\mu)^{2(d-4)} \left\{ \frac{\Lambda^2}{2} \Gamma_i \eta_a^i O_a(x) + \frac{\Lambda}{(4\pi)^2} [\beta_a O_a(x) + (4\pi)^2 L_i^r(\mu, d) \eta_a^i O_a(x)] \right. \\
&+ \frac{1}{(4\pi)^4} \left[-\frac{1}{8} \ln^2 M^2/\mu^2 \Gamma_i \eta_a^i O_a(x) + \frac{1}{2} \ln M^2/\mu^2 (4\pi)^2 L_i^r(\mu, 4) \eta_a^i O_a(x) \right. \\
&+ \ln M^2/\mu^2 \beta_a O_a(x) + H_i(x, 4; M) \left((4\pi)^2 L_i^r(\mu, 4) - \frac{\Gamma_i}{2} \ln M^2/\mu^2 \right) \\
&\left. + E(x; M) + \Gamma_i H_i'(x, 4; M) \right] + O(d-4) \left. \right\} .
\end{aligned} \tag{A.13}$$

The functional $H_i'(x, 4; M)$ is defined by the Taylor expansion

$$H_i(x, d; M) = H_i(x, 4; M) + (d-4) H_i'(x, 4; M) + O[(d-4)^2] \tag{A.14}$$

and it is scale independent because of Eq. (A.8).

Now we can render the complete functional finite by adding the tree-level functional of $O(p^6)$ (in the notation of Eq. (4.9) in Ref. [4]):

$$\begin{aligned} Z_6^g &= \int d^d x C_a(d) O_a(x) \\ &= \int d^d x (c\mu)^{2(d-4)} \left[C_a^r(\mu, d) - \frac{\Gamma_a^{(2)}}{F^2} \Lambda^2 - \frac{1}{F^2} \left(\Gamma_a^{(1)} + \Gamma_a^{(L)}(\mu, d) \right) \Lambda \right] O_a(x). \end{aligned} \quad (\text{A.15})$$

Comparing Eqs. (A.13) and (A.15), the divergences are canceled with

$$\Gamma_a^{(2)} = \frac{F^2}{2} \Gamma_i \eta_a^i, \quad \Gamma_a^{(1)} = \frac{F^2}{(4\pi)^2} \beta_a, \quad \Gamma_a^{(L)}(\mu, d) = F^2 L_i^r(\mu, d) \eta_a^i. \quad (\text{A.16})$$

The coefficients $\Gamma_a^{(1)}$, $\Gamma_a^{(2)}$, $\Gamma_a^{(L)}(\mu, d)$ are listed in Table II of App. C in Ref. [4].

Summing up the diagrams a, b, d and g, the limit $d \rightarrow 4$ can now be taken to arrive at the final result

$$\begin{aligned} Z_6^{a+b+d+g} &= \int d^4 x \left\{ C_a^r(\mu) O_a(x) + \frac{1}{4F^2} \left(4\Gamma_a^{(1)} L(\mu) - \Gamma_a^{(2)} L^2(\mu) + 2\Gamma_a^{(L)}(\mu) L(\mu) \right) O_a(x) \right. \\ &\quad \left. + \frac{1}{(4\pi)^2} \left[L_i^r(\mu) - \frac{\Gamma_i}{2} L(\mu) \right] H_i(x; M) + \frac{1}{(4\pi)^4} K(x; M) \right\} \end{aligned} \quad (\text{A.17})$$

with the chiral log $L(\mu)$ defined in Eq. (2.2) and with

$$\begin{aligned} C_a^r(\mu) &= C_a^r(\mu, 4), \quad L_i^r(\mu) = L_i^r(\mu, 4), \quad \Gamma_a^{(L)}(\mu) = \Gamma_a^{(L)}(\mu, 4) \\ H_i(x; M) &= H_i(x, 4; M), \quad K(x; M) = E(x; M) + \Gamma_i H_i'(x, 4; M). \end{aligned} \quad (\text{A.18})$$

The scale dependence is contained in $C_a^r(\mu)$, $L_i^r(\mu)$, $L(\mu)$. The functionals $O_a(x)$, $H_i(x; M)$ and $K(x; M)$ are independent of μ . Scale independence of the complete functional (A.17) can be checked with the help of the renormalization group equations (4.5) in Ref. [4]:

$$\mu \frac{dC_a^r(\mu)}{d\mu} = \frac{1}{(4\pi)^2 F^2} \left[2\Gamma_a^{(1)} + \Gamma_a^{(L)}(\mu) \right]. \quad (\text{A.19})$$

As already mentioned, the sum of reducible diagrams c, e, f is finite and scale independent by itself. It can be written in the form

$$\begin{aligned} Z_6^{c+e+f} &= \int d^4 x d^4 y \left[\left(L_i^r(\mu) - \frac{\Gamma_i}{2} L(\mu) \right) P_{i,\alpha}(x) + F_\alpha(x; M) \right] G_{\alpha,\beta}(x, y) \\ &\quad \times \left[\left(L_j^r(\mu) - \frac{\Gamma_j}{2} L(\mu) \right) P_{j,\beta}(y) + F_\beta(y; M) \right]. \end{aligned} \quad (\text{A.20})$$

The derivatives of the monomials $P_i(x)$ defining the chiral Lagrangian of $O(p^4)$ with respect to the fields φ_α ($\alpha = 1, \dots, 8$) are denoted $P_{i,\alpha}(x)$. The $F_\alpha(x; M)$ are finite and scale independent one-loop functionals. The propagator $G_{\alpha,\beta}(x, y)$ is again a functional of the classical field. Although the functional (A.20) is nonlocal in general, it contributes in many cases of interest to wave function, mass and decay constant renormalization only.

The complete generating functional of $O(p^6)$ is then given by the sum

$$Z_6 = Z_6^{a+b+d+g} + Z_6^{c+e+f}. \quad (\text{A.21})$$

Once again, it is independent of both scales μ and M .

B Approximation II for F_K/F_π

The original Approximation I for F_K/F_π was given in the appendix of Ref. [3]. In Approximation II discussed in Sec. 3, there is an additional contribution of $O(p^6)$ denoted R_6^{ext} below. The complete result for F_K/F_π is

$$F_K/F_\pi = 1 + R_4 + R_6 + R_6^{\text{ext}}, \quad (\text{B.1})$$

$$F_0^2 R_4 = 4(\dot{M}_K^2 - \dot{M}_\pi^2) L_5 - 5\bar{A}(\dot{M}_\pi, \mu)/8 + \bar{A}(\dot{M}_K, \mu)/4 + 3\bar{A}(\dot{M}_\eta, \mu)/8, \quad (\text{B.2})$$

$$\begin{aligned} F_0^4 R_6 &= 8F_0^2(\dot{M}_K^2 - \dot{M}_\pi^2) \left(2\dot{M}_K^2 (C_{14} + C_{15}) + \dot{M}_\pi^2 (C_{15} + 2C_{17}) \right) \\ &+ (\dot{M}_K^2 - \dot{M}_\pi^2) \left(-32(\dot{M}_\pi^2 + 2\dot{M}_K^2)L_4 L_5 - 8(3\dot{M}_\pi^2 + \dot{M}_K^2)L_5^2 \right. \\ &\quad \left. + (25\dot{M}_\pi^2 + 17\dot{M}_K^2)L^2/32 \right) \\ &+ \frac{(\dot{M}_K^2 - \dot{M}_\pi^2)}{(4\pi)^2} \left(-2(\dot{M}_\pi^2 + \dot{M}_K^2)L_1 - (\dot{M}_\pi^2 + \dot{M}_K^2)L_2 - (5\dot{M}_\pi^2 + \dot{M}_K^2)L_3/18 \right. \\ &\quad \left. + 6(\dot{M}_\pi^2 + 2\dot{M}_K^2)L_4 + (14\dot{M}_\pi^2 + 22\dot{M}_K^2)L_5/3 - 12(\dot{M}_\pi^2 + 2\dot{M}_K^2)L_6 \right. \\ &\quad \left. + 16(\dot{M}_\pi^2 - \dot{M}_K^2)L_7 - 4(\dot{M}_\pi^2 + 5\dot{M}_K^2)L_8 + (313\dot{M}_\pi^2 + 271\dot{M}_K^2)L/288 \right) \\ &+ 5\bar{A}(\dot{M}_\pi, \mu)^2/8 - \bar{A}(\dot{M}_K, \mu)^2/8 + \bar{A}(\dot{M}_\pi, \mu)\bar{A}(\dot{M}_K, \mu)/16 \\ &- 3\bar{A}(\dot{M}_\pi, \mu)\bar{A}(\dot{M}_\eta, \mu)/8 - 3\bar{A}(\dot{M}_K, \mu)\bar{A}(\dot{M}_\eta, \mu)/16 \\ &+ \bar{A}(\dot{M}_\pi, \mu) \left(4\dot{M}_\pi^2 L_1 + 10\dot{M}_\pi^2 L_2 + 13\dot{M}_\pi^2 L_3/2 + 10(\dot{M}_\pi^2 + 2\dot{M}_K^2)L_4 \right. \\ &\quad \left. + (19\dot{M}_\pi^2 - 5\dot{M}_K^2)L_5/2 - 10(\dot{M}_\pi^2 + 2\dot{M}_K^2)L_6 - 10\dot{M}_\pi^2 L_8 \right. \\ &\quad \left. - (361\dot{M}_\pi^2 + 131\dot{M}_K^2)L/288 \right) \\ &+ \bar{A}(\dot{M}_K, \mu) \left(-4\dot{M}_K^2 L_1 - 10\dot{M}_K^2 L_2 - 5\dot{M}_K^2 L_3 - 4(\dot{M}_\pi^2 + 2\dot{M}_K^2)L_4 \right. \\ &\quad \left. - (\dot{M}_\pi^2 + \dot{M}_K^2)L_5 + 4(\dot{M}_\pi^2 + 2\dot{M}_K^2)L_6 + 4\dot{M}_K^2 L_8 + (59\dot{M}_\pi^2 + 115\dot{M}_K^2)L/144 \right) \\ &+ \bar{A}(\dot{M}_\eta, \mu)(\dot{M}_K^2 - \dot{M}_\pi^2)/\dot{M}_\eta^2 \left(-9\dot{M}_\pi^2 L_7 - 3\dot{M}_\pi^2 L_8 + 5\dot{M}_\pi^2 L/32 \right) \\ &+ \bar{A}(\dot{M}_\eta, \mu) \left((\dot{M}_\pi^2/2 - 2\dot{M}_K^2)L_3 - 6(\dot{M}_\pi^2 + 2\dot{M}_K^2)L_4 - (7\dot{M}_\pi^2 + 23\dot{M}_K^2)L_5/6 \right. \\ &\quad \left. + 6(\dot{M}_\pi^2 + 2\dot{M}_K^2)L_6 + 3(3\dot{M}_\pi^2\dot{M}_K^2/\dot{M}_\eta^2 - 7\dot{M}_\pi^2 + 4\dot{M}_K^2)L_7 \right. \\ &\quad \left. + 3(\dot{M}_\pi^2\dot{M}_K^2/\dot{M}_\eta^2 - 3\dot{M}_\pi^2 + 4\dot{M}_K^2)L_8 \right. \\ &\quad \left. - (15\dot{M}_\pi^2\dot{M}_K^2/\dot{M}_\eta^2 - 44\dot{M}_\pi^2 - 19\dot{M}_K^2)L/96 \right), \quad (\text{B.3}) \end{aligned}$$

$$\begin{aligned}
F_0^4 R_6^{\text{ext}} &= -\frac{(\mathring{M}_K^2 - \mathring{M}_\pi^2)}{(4\pi)^2} (17\mathring{M}_K^2 + 10\mathring{M}_\pi^2) L/48 - (\mathring{M}_K^2 - \mathring{M}_\pi^2) (11\mathring{M}_K^2 + 7\mathring{M}_\pi^2) L^2/96 \\
&+ \frac{(\mathring{M}_K^2 - \mathring{M}_\pi^2)}{(4\pi)^2} (10\mathring{M}_K^2 + 17\mathring{M}_\pi^2)/4608 + \frac{(\mathring{M}_K^2 - \mathring{M}_\pi^2)}{(4\pi)^4} (17\mathring{M}_K^2 + 19\mathring{M}_\pi^2)/384 \\
&+ \bar{A}(\mathring{M}_\pi, \mu) \left\{ -(35\mathring{M}_\pi^2 + 49\mathring{M}_K^2) L/288 + \frac{1}{(4\pi)^2} (8\mathring{M}_\pi^2 + \mathring{M}_K^2)/32 \right\} \\
&- \bar{A}(\mathring{M}_\pi, \mu)^2 (19 + 20\mathring{M}_K^2/\mathring{M}_\pi^2)/128 + 3\bar{A}(\mathring{M}_\pi, \mu)\bar{A}(\mathring{M}_K, \mu)/32 \\
&+ \bar{A}(\mathring{M}_\pi, \mu)\bar{A}(\mathring{M}_\eta, \mu) (7 + 36\mathring{M}_\pi^2/\mathring{M}_\eta^2)/192 \\
&+ \bar{A}(\mathring{M}_K, \mu) \left\{ (121\mathring{M}_\pi^2 - 115\mathring{M}_K^2) L/144 + \frac{1}{(4\pi)^2} (-4\mathring{M}_\pi^2 + 7\mathring{M}_K^2)/16 \right\} \\
&+ \bar{A}(\mathring{M}_K, \mu)^2 (3 + 10\mathring{M}_\pi^2/\mathring{M}_K^2)/32 - \bar{A}(\mathring{M}_K, \mu)\bar{A}(\mathring{M}_\eta, \mu) (71 + 12\mathring{M}_\pi^2/\mathring{M}_\eta^2)/96 \\
&+ \bar{A}(\mathring{M}_\eta, \mu) \left\{ (-12\mathring{M}_\pi^2\mathring{M}_K^2/\mathring{M}_\eta^2 - 23\mathring{M}_\pi^2 + 18\mathring{M}_\pi^4/\mathring{M}_\eta^2 + 41\mathring{M}_K^2) L/96 \right. \\
&\quad \left. + \frac{1}{(4\pi)^2} (4\mathring{M}_\pi^2 - 19\mathring{M}_K^2)/32 \right\} + \bar{A}(\mathring{M}_\eta, \mu)^2 (56 + \mathring{M}_\pi^2/\mathring{M}_\eta^2)/128 . \tag{B.4}
\end{aligned}$$

We use $L_i = L_i^r(\mu)$, $C_a = C_a^r(\mu)$, $L = L(\mu)$ for a compact representation. The masses \mathring{M}_α are the lowest-order meson masses of $O(p^2)$. Since we work to $O(p^6)$, substituting the lowest-order masses \mathring{M}_α by the actual lattice masses generates an additional contribution of $O(p^6)$ [6]. F_0 is the meson decay constant in the chiral $SU(3)$ limit and the chiral log L is defined in Eq. (2.2). The loop function $\bar{A}(M_\alpha, \mu)$ is defined as

$$\bar{A}(M_\alpha, \mu) = \frac{M_\alpha^2}{(4\pi)^2} \ln \frac{\mu^2}{M_\alpha^2} . \tag{B.5}$$

C Approximation I for F_π

In the approximation defined by the functional (2.1), F_π assumes the form

$$\begin{aligned}
F_\pi &= F_0 \\
&+ F_0^{-1} \left\{ 4(2\mathring{M}_K^2 + \mathring{M}_\pi^2) L_4 + 4\mathring{M}_\pi^2 L_5 + \bar{A}(\mathring{M}_\pi, \mu) + \bar{A}(\mathring{M}_K, \mu)/2 \right\} \\
&+ F_0^{-1} \left\{ 8\mathring{M}_\pi^4 (C_{14} + C_{15} + 3C_{16} + C_{17}) + 16\mathring{M}_\pi^2 \mathring{M}_K^2 (C_{15} - 2C_{16}) + 32\mathring{M}_K^4 C_{16} \right\} \\
&+ \frac{F_0^{-3}}{(4\pi)^2} (284\mathring{M}_\pi^2 \mathring{M}_K^2 + 525\mathring{M}_\pi^4 + 608\mathring{M}_K^4) L/288 \\
&+ F_0^{-3} (-34\mathring{M}_\pi^2 \mathring{M}_K^2 + 185\mathring{M}_\pi^4 + 164\mathring{M}_K^4) L^2/144 \\
&+ \frac{F_0^{-3}}{(4\pi)^2} \left\{ -2\mathring{M}_\pi^4 L_1 + (8\mathring{M}_\pi^2 \mathring{M}_K^2 - 37\mathring{M}_\pi^4 - 52\mathring{M}_K^4) L_2/9 \right. \\
&\quad + (8\mathring{M}_\pi^2 \mathring{M}_K^2 - 28\mathring{M}_\pi^4 - 43\mathring{M}_K^4) L_3/27 + 4(5\mathring{M}_\pi^2 \mathring{M}_K^2 + 2\mathring{M}_\pi^4 + 2\mathring{M}_K^4) L_4 \\
&\quad \left. + 4(2\mathring{M}_\pi^4 + \mathring{M}_K^4) L_5 - 8(5\mathring{M}_\pi^2 \mathring{M}_K^2 + 2\mathring{M}_\pi^4 + 2\mathring{M}_K^4) L_6 - 8(2\mathring{M}_\pi^4 + \mathring{M}_K^4) L_8 \right\} \\
&+ F_0^{-3} \left\{ -8(4\mathring{M}_\pi^2 \mathring{M}_K^2 + \mathring{M}_\pi^4 + 4\mathring{M}_K^4) L_4^2 - 16(2\mathring{M}_\pi^2 \mathring{M}_K^2 + \mathring{M}_\pi^4) L_4 L_5 - 8\mathring{M}_\pi^4 L_5^2 \right\} \\
&+ F_0^{-3} \bar{A}(\mathring{M}_\pi, \mu) \left\{ -28\mathring{M}_\pi^2 L_1 - 16\mathring{M}_\pi^2 L_2 - 14\mathring{M}_\pi^2 L_3 - 24\mathring{M}_K^2 L_4 \right. \\
&\quad \left. - 6\mathring{M}_\pi^2 L_5 + 16(\mathring{M}_\pi^2 + 2\mathring{M}_K^2) L_6 + 16\mathring{M}_\pi^2 L_8 + (359\mathring{M}_\pi^2 + 40\mathring{M}_K^2) L/144 \right\} \\
&+ F_0^{-3} \bar{A}(\mathring{M}_K, \mu) \left\{ -32\mathring{M}_K^2 L_1 - 8\mathring{M}_K^2 L_2 - 10\mathring{M}_K^2 L_3 + 2(-3\mathring{M}_\pi^2 + 2\mathring{M}_K^2) L_4 \right. \\
&\quad \left. + 2(\mathring{M}_\pi^2 - 2\mathring{M}_K^2) L_5 + 8(\mathring{M}_\pi^2 + 2\mathring{M}_K^2) L_6 + 8\mathring{M}_K^2 L_8 + (-11\mathring{M}_\pi^2 + 62\mathring{M}_K^2) L/36 \right\} \\
&+ F_0^{-3} \bar{A}(\mathring{M}_\eta, \mu) \left\{ 8(\mathring{M}_\pi^2 - 4\mathring{M}_K^2) L_1/3 + 2(\mathring{M}_\pi^2 - 4\mathring{M}_K^2) L_2/3 + 2(\mathring{M}_\pi^2 - 4\mathring{M}_K^2) L_3/3 \right. \\
&\quad \left. + 4(-\mathring{M}_\pi^2 + 4\mathring{M}_K^2) L_4/3 + 2\mathring{M}_\pi^2 L_5/3 + (-11\mathring{M}_\pi^2 + 20\mathring{M}_K^2) L/48 \right\} . \tag{C.1}
\end{aligned}$$

The notation is as in App. B.

References

- [1] S. Aoki *et al.*, Review of lattice results concerning low energy particle physics, arXiv:1310.8555 [hep-lat].
- [2] J. Bijnens, Prog. Part. Nucl. Phys. **58** (2007) 521 [hep-ph/0604043].
- [3] G. Ecker, P. Masjuan and H. Neufeld, Phys. Lett. B **692** (2010) 184 [arXiv:1004.3422 [hep-ph]].

- [4] J. Bijnens, G. Colangelo and G. Ecker, *Annals Phys.* **280** (2000) 100 [hep-ph/9907333].
- [5] J. Gasser and H. Leutwyler, *Annals Phys.* **158** (1984) 142.
- [6] J. Gasser and H. Leutwyler, *Nucl. Phys. B* **250** (1985) 465.
- [7] J. Bijnens, G. Colangelo and G. Ecker, *JHEP* **9902** (1999) 020 [hep-ph/9902437].
- [8] J. Bijnens, G. Colangelo and G. Ecker, *Phys. Lett. B* **441** (1998) 437 [hep-ph/9808421].
- [9] G. Amorós, J. Bijnens and P. Talavera, *Nucl. Phys. B* **568** (2000) 319 [hep-ph/9907264].
- [10] V. Bernard and E. Passemar, *JHEP* **1004** (2010) 001 [arXiv:0912.3792 [hep-ph]] and private communication.
- [11] S. Dürr *et al.* [BMW Collaboration], *Phys. Rev. D* **81** (2010) 054507 [arXiv:1001.4692 [hep-lat]].
- [12] G. Amorós, J. Bijnens and P. Talavera, *Nucl. Phys. B* **602** (2001) 87 [hep-ph/0101127].
- [13] J. Bijnens and I. Jemos, *Nucl. Phys. B* **854** (2012) 631 [arXiv:1103.5945 [hep-ph]].
- [14] J. Gasser, C. Haefeli, M. A. Ivanov and M. Schmid, *Phys. Lett. B* **652** (2007) 21 [arXiv:0706.0955 [hep-ph]].
- [15] Y. Aoki *et al.* [RBC and UKQCD Collaborations], *Phys. Rev. D* **83** (2011) 074508 [arXiv:1011.0892 [hep-lat]].
- [16] R. Arthur *et al.* [RBC and UKQCD Collaborations], *Phys. Rev. D* **87** (2013) 094514 [arXiv:1208.4412 [hep-lat]].
- [17] J. Beringer *et al.* [Particle Data Group Collaboration], *Phys. Rev. D* **86** (2012) 010001.
- [18] S. Descotes-Genon, L. Girlanda and J. Stern, *JHEP* **0001** (2000) 041 [hep-ph/9910537].
- [19] A. Bazavov *et al.*, *Rev. Mod. Phys.* **82** (2010) 1349 [arXiv:0903.3598 [hep-lat]].
- [20] M. Ademollo and R. Gatto, *Phys. Rev. Lett.* **13** (1964) 264.
- [21] J. Gasser and H. Leutwyler, *Nucl. Phys. B* **250** (1985) 517.
- [22] A. Bazavov *et al.* [Fermilab Lattice and MILC Collaborations], *Phys. Rev. D* **87** (2013) 073012 [arXiv:1212.4993 [hep-lat]].
- [23] P. A. Boyle *et al.* [RBC and UKQCD Collaborations], *JHEP* **1308** (2013) 132 [arXiv:1305.7217 [hep-lat]].
- [24] P. Post and K. Schilcher, *Eur. Phys. J. C* **25** (2002) 427 [hep-ph/0112352].
- [25] J. Bijnens and P. Talavera, *Nucl. Phys. B* **669** (2003) 341 [hep-ph/0303103].
- [26] S. Weinberg, *Physica A* **96** (1979) 327.